

A density functional theory study of the correlation between analyte basicity, ZnPc adsorption strength, and sensor response

N. L. Tran, F. I. Bohrer, W. C. Trogler, and A. C. Kummel^{a)}

*Department of Chemistry and Biochemistry, University of California, San Diego,
La Jolla, California 92039-0358, USA*

(Received 4 January 2009; accepted 27 April 2009; published online 28 May 2009)

Density functional theory (DFT) simulations were used to determine the binding strength of 12 electron-donating analytes to the zinc metal center of a zinc phthalocyanine molecule (ZnPc monomer). The analyte binding strengths were compared to the analytes' enthalpies of complex formation with boron trifluoride (BF₃), which is a direct measure of their electron donating ability or Lewis basicity. With the exception of the most basic analyte investigated, the ZnPc binding energies were found to correlate linearly with analyte basicities. Based on natural population analysis calculations, analyte complexation to the Zn metal of the ZnPc monomer resulted in limited charge transfer from the analyte to the ZnPc molecule, which increased with analyte-ZnPc binding energy. The experimental analyte sensitivities from chemiresistor ZnPc sensor data were proportional to an exponential of the binding energies from DFT calculations consistent with sensitivity being proportional to analyte coverage and binding strength. The good correlation observed suggests DFT is a reliable method for the prediction of chemiresistor metallophthalocyanine binding strengths and response sensitivities. © 2009 American Institute of Physics. [DOI: 10.1063/1.3134743]

I. INTRODUCTION

Metallophthalocyanines (MPcs) are porphyrin analogs that can form highly ordered, chemically inert, and thermally stable films. They have been studied extensively with both experimental and theoretical techniques.¹⁻⁹ More than 70 phthalocyanines with varying electronic properties have been synthesized, since their chemical properties can be easily manipulated by changing the metal center or substituting functional groups to the organic rings.¹⁰ Their stability and widely varying chemical properties make them an attractive candidate for use in chemical sensors. Bott and Jones¹¹ showed that two-terminal resistive sensors with different *p*-type MPc films (metal-free H₂Pc, PbPc, CoPc, CuPc, NiPc, MgPc, and ZnPc) are sensitive to the strong oxidants NO₂ and Cl₂ at low parts per million concentrations. A study by Bohrer *et al.*^{12,13} revealed that arrays of two-terminal MPc sensors could be used to selectively distinguish between 12 nonoxidizing Lewis base analytes with varying chemical properties. In addition, Yang *et al.*¹⁴ directly compared the effect of strong and weak binding donor analytes to *p*-type and *n*-type phthalocyanine-based three-terminal field effect MPc transistor sensors. Although the experimental literature pertaining to MPc sensor applications is extensive, most experimental studies focus on the sensor responses of one or two analyte vapors onto multiple MPcs.^{15,16}

Existing theoretical investigations of MPcs have focused primarily on the electronic structure of an isolated, single molecule MPc (monomer),^{2,17,18} the analyte-free film in its β -crystalline form,¹⁹ or the molecular interaction of the MPc monomer with a MPc substrate.²⁰ Several computational

studies have investigated the interaction of an analyte with the MPc, but most of these studies are focused either on analyte binding to the hydrogen bridge of the metal-free phthalocyanine²¹ or the binding of a single analyte onto the metal center of the MPc.²² Another computational study reported the binding of an electron donating analyte and electron accepting analyte to FePc at seven different plausible binding sites on the FePc molecule, but only two analytes were studied.²³ To our knowledge, there have been no published theoretical studies examining the binding strength of a variety of gaseous analytes to a MPc monomer.

This study attempts to investigate the adsorption strength of 12 analytes spanning a wide range of Lewis basicities based on the $-\Delta H_{\text{BF}_3}$ scale to the Zn metal of the ZnPc monomer using density functional theory (DFT).²⁴ The $-\Delta H_{\text{BF}_3}$ scale is an indicator of the ability of an analyte to donate electrons and is an enthalpy scale based on the stoichiometric 1:1 formation of an electron donor with BF₃. The simulated binding strengths to ZnPc are compared to their enthalpy of formation with BF₃. The DFT calculated binding strengths are also compared to current response data from a recent sensor study using chemiresistive ZnPc sensors by Bohrer *et al.*¹² Finally, charge transfer on analyte binding was also investigated using natural population analysis (NPA) calculations.

II. COMPUTATIONAL METHODS

Optimizations of all systems—the ZnPc monomer, all analytes, and the ZnPc-analyte complexes—were performed using GAUSSIAN03, revision D.01 with the Becke three-parameter hybrid exchange functional and Lee–Yang–Parr gradient corrected electron correlation functional (B3LYP)

^{a)}Electronic mail: akummel@ucsd.edu.

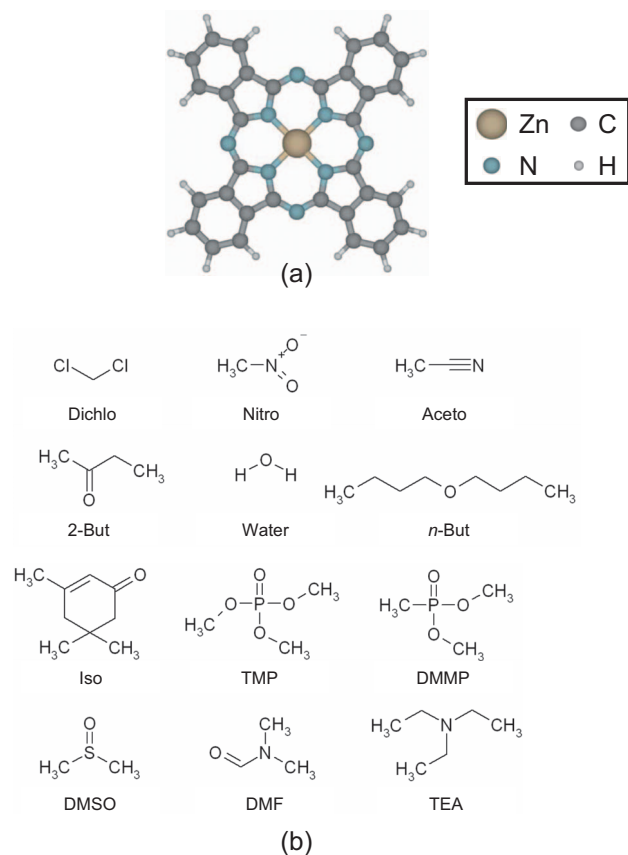


FIG. 1. (Color) Schematic of (a) an isolated, single molecule zinc phthalocyanine molecule (b) all 12 electron donating analytes studied.

with the 6-31G* basis.^{25–29} Several studies have shown that hybrid functionals are a computationally cost effective and yet reliable method to predict the molecular geometry and electronic structure of MPcs.^{30–32} Whereas localized and semilocalized functionals [local-density approximation/generalized-gradient approximation (GGA)] could have also been used to accurately predict MPC molecular geometry, their shortcomings in modeling the electronic structure of extended systems are well documented.³⁰ All initial structures were built using GAUSSVIEW, version 2.08.³³ A schematic of the ZnPc monomer and the analytes studied can be found in Figs. 1(a) and 1(b), respectively. The bond lengths and bond angles of the calculated ground state structures for ZnPc (D_{4h}),^{18,34} dichloromethane (dichlo),³⁵ nitromethane (nitro),³⁶ acetonitrile (aceto),^{37,38} *cis*-2-butanone (2-but),³⁹ water, di-*n*-butylether (*n*-but),⁴⁰ trimethylphosphate (TMP),⁴¹ dimethylmethylphosphonate (DMMP),⁴² isophorone (iso),⁴³ dimethylsulfoxide (DMSO),⁴⁴ *N,N*-dimethylformamide (DMF),⁴⁵ and triethylamine (TEA)^{46,47} agree with those determined by other computational and experimental studies to within 0.03 Å and 0.02°.

Only binding to the Zn metal center of the ZnPc monomer was investigated since numerous experimental and theoretical studies have shown that preferential binding occurs to the metal center.^{23,48,49} Additionally, experimental sensor data show the response differs for a given analyte on different MPC films consistent with bonding to the metal centers.⁵⁰ Various initial geometries of analyte binding to the Zn metal center were sampled to determine the lowest energy binding

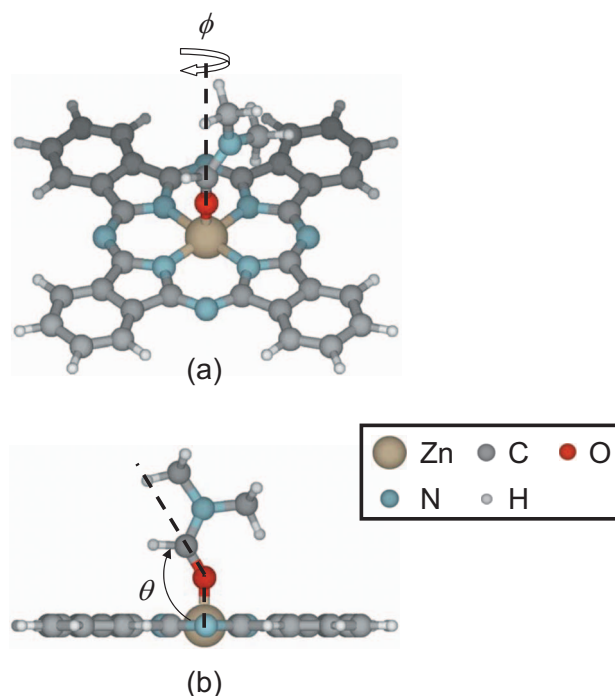


FIG. 2. (Color) Schematic of the initial geometry of two of more than eight conformational isomers sampled for DMF binding to ZnPc. (a) Double-bonded oxygen atom of DMF binding to the Zn metal where the torsional angle $\phi=0^\circ$ is formed by the C–N bond lying in the DMF molecular plane eclipsing the Zn–N bond of the ZnPc molecule. Other ZnPc–DMF isomers consist of rotating the DMF molecule by 45° about this torsional angle ϕ ; the configuration rotated by 45° will be referred to as “staggered.” (b) Side view of DMF binding to the Zn metal where the DMF molecule is staggered with respect to the Zn–N bond. The DMF molecule is bonded such that the Zn–O–C angle θ is 150° . The remaining ZnPc–DMF isomers are formed by varying θ at 15° increments from 180° to 135° .

conformation for each analyte. For example, eight conformational isomers were investigated for the binding of DMF to the ZnPc metal center via the oxygen atom of the DMF molecule; Fig. 2 shows the initial geometry of two of the more than eight conformations investigated for the ZnPc–DMF complex. Figure 2(a) shows DMF binding through the double-bonded oxygen atom of DMF to the Zn metal of the ZnPc monomer. In this figure, the backbone of the DMF molecule eclipses the Zn–N bond of the ZnPc molecule to give a torsional angle $\phi=0^\circ$, while the Zn–O–C angle is linear with $\theta=180^\circ$. Three other ZnPc–DMF conformations sampled included variations in θ at 15° increments ($\theta = 165^\circ, 150^\circ, \text{ and } 135^\circ$). The remaining four complexes sampled involve rotating the DMF molecule by 45° about ϕ in conjunction with varying θ at 15° increments from 180° to 135° . Figure 2(b) shows a side view of DMF binding to the Zn metal where $\phi=45^\circ$ and $\theta=150^\circ$. The variations in ϕ and θ sampled for DMF binding to the Zn metal oxygen-end down resulted in a small range of enthalpies from -34.46 to -35.87 kJ/mol exothermic. Of the eight DMF–ZnPc conformations studied, only two contained no imaginary frequencies. The most stable conformation (-35.9 kJ/mol exothermic) with no imaginary frequencies contains $\phi=45^\circ$ and $\theta=122^\circ$ and can be found in the AIP’s Electronic Physics Auxiliary Publication Service (EPAPS) depository.⁵¹ Binding through the nitrogen atom of the DMF molecule to the Zn

metal of the ZnPc monomer was also investigated. This was endothermic, therefore, sampling other conformations of DMF binding to the Zn metal via the nitrogen atom was subsequently abandoned.

While binding through both the nitrogen and oxygen atoms was sampled for DMF bonding to ZnPc, only binding via the nitrogen atom was investigated for acetonitrile (aceto) and TEA since they have no other basic lone electron pairs. For *cis*-2-butanone (2-but), water, *n*-butylether (*n*-but), and isophorone (iso), only binding through the oxygen atom was sampled since they have no other viable lone pairs. For TMP and DMMP, only binding through the more basic oxygen double bonded to the phosphorous was investigated. For DMSO, binding through both the oxygen and the electron rich sulfur was sampled; DMSO binding through the double-bonded oxygen atom was found to be -38.59 kJ/mol exothermic whereas binding through the sulfur atom was endothermic. In all cases, geometry optimizations of numerous ZnPc-analyte complexes were investigated to determine the lowest binding energy conformational isomer for each analyte.

For TEA, additional molecular dynamics (MD) simulations using the Vienna *ab initio* simulations package (VASP) (Refs. 52–54) were used in an attempt to locate the global minimum ZnPc-TEA binding conformation since the ZnPc-TEA complex contains a large number of degrees freedom (231) compared to all other ZnPc-analyte complexes. Prior to beginning the MD simulations, geometry optimizations of two of the lowest energy or most stable conformations of the ZnPc-TEA complex as determined from GAUSSIAN03 were performed using VASP with the PW91 variety of the GGA using ultrasoft Vanderbilt pseudopotentials as supplied within VASP^{54–56} and a single *k*-point (located at the gamma point). The kinetic energy cutoff was set to 400 eV. All three systems were geometrically relaxed to a convergence tolerance of 0.01 eV/Å. The two VASP-optimized ZnPc-TEA complexes were heated to 150 K for 1 ps followed by cooling to 0 K over a 1 ps period. Once the MD simulations were complete, the structures from the last time step were reoptimized in G03 for a consistent and proper comparison of binding energies with respect to all other analytes studied.

All systems were verified to be minima by evaluating the Hessian matrix in G03. Only complexes containing no imaginary frequencies are discussed in this study. The binding energies (ΔE_{bind}) were calculated as

$$\Delta E_{\text{bind}} = E(\text{ZnPc} + \text{analyte}) - E(\text{ZnPc}) - E(\text{analyte}), \quad (1)$$

where $E(\text{ZnPc} + \text{analyte})$, $E(\text{ZnPc})$, and $E(\text{analyte})$ represent the total energies of the ZnPc-analyte complex, the gas-phase ZnPc, and the gas-phase analyte, respectively. All binding energies discussed include the correction for the zero-point vibrational energy (ZPE). The ZPE correction (ΔE_{ZPE}) is calculated as

$$\Delta E_{\text{ZPE}} = E_{\text{ZPE}}(\text{ZnPc} + \text{analyte}) - E_{\text{ZPE}}(\text{ZnPc}) - E_{\text{ZPE}}(\text{analyte}), \quad (2)$$

TABLE I. Analytes and their $-\Delta H_{\text{BF}_3}$ enthalpy values. Abbreviations: Dichlo=dichloromethane, Nitro=nitromethane, Aceto=acetonitrile, 2-but=2-butanone, *n*-but=di-*n*-butylether, Iso=isophorone, TMP=trimethylphosphate, DMMP=dimethylmethylphosphonate, DMSO=dimethylsulfoxide, DMF=*N,N*-dimethylformamide, and TEA=triethylamine.

Gas analytes	$-\Delta H_{\text{BF}_3}$ (kJ/mol) ^a
Dichlo	10 ± 0.03
Nitro	37.63 ± 0.56
Aceto	60.39 ± 0.46
2-but	76.07 ± 0.33
Water ^a	82.1 ± 4.3
<i>n</i> -but	78.57 ± 0.39
Iso ^b	78.76 ± 0.41
TMP	84.79 ± 0.22
DMMP ^a	104.0 ± 12.9
DMSO	105.34 ± 0.36
<i>N,N</i> -DMF	110.49 ± 0.35
TEA	135.87 ± 1.67

^aAll values listed are from Ref. 24 except for water and DMMP which were extrapolated from ZnPc sensor data in Ref. 12.

^bThe basicity value listed for isophorone has been corrected for binding through the alkene (Refs. 13 and 55).

where $E_{\text{ZPE}}(\text{ZnPc} + \text{analyte})$, $E_{\text{ZPE}}(\text{ZnPc})$, and $E_{\text{ZPE}}(\text{analyte})$ represent the ZPE correction for the ZnPc-analyte complex, the gas-phase ZnPc, and the gas-phase analyte, respectively. Counterpoise corrections using the Boys and Bernardi counterpoise correction scheme as supplied within GAUSSIAN 03 were also included to account for basis set superposition errors (BSSEs).^{57,58}

The BSSE correction (ΔE_{BSSE}) is calculated as

$$\Delta E_{\text{BSSE}} = E_{\text{BSSE}}(\text{ZnPc} + \text{analyte}) - E_{\text{BSSE}}(\text{ZnPc}) - E_{\text{BSSE}}(\text{analyte}), \quad (3)$$

where $E_{\text{BSSE}}(\text{ZnPc} + \text{analyte})$, $E_{\text{BSSE}}(\text{ZnPc})$, and $E_{\text{BSSE}}(\text{analyte})$ represent the BSSE correction energy for the ZnPc-analyte complex, the gas-phase ZnPc fragment, and the gas-phase analyte fragment, respectively. Therefore, the ZPE and BSSE corrected binding energies ($\Delta E_{\text{bind}}^{\text{corr}}$) are simply calculated as

$$\Delta E_{\text{bind}}^{\text{corr}} = \Delta E_{\text{bind}} + \Delta E_{\text{ZPE}} + \Delta E_{\text{BSSE}}. \quad (4)$$

Only $\Delta E_{\text{bind}}^{\text{corr}}$ energies will be discussed in this paper.

III. RESULTS AND DISCUSSION

A. ZnPc binding versus Lewis basicity

Table I lists the 12 analytes studied along with their Lewis basicities based on the $-\Delta H_{\text{BF}_3}$ scale where dichloromethane is the weakest base with $-\Delta H_{\text{BF}_3} = 10 \pm 0.03$ kJ/mol and TEA is the strongest ($-\Delta H_{\text{BF}_3} = 135.87 \pm 1.67$ kJ/mol).²⁴ Note that the $-\Delta H_{\text{BF}_3}$ enthalpy value listed for isophorone has been corrected by 11.8 kJ/mol since its enthalpy value has been overestimated due to the ability of BF_3 to bind the alkene as well as the oxygen atom.^{13,59} Additionally, Lewis basicity values for DMMP and

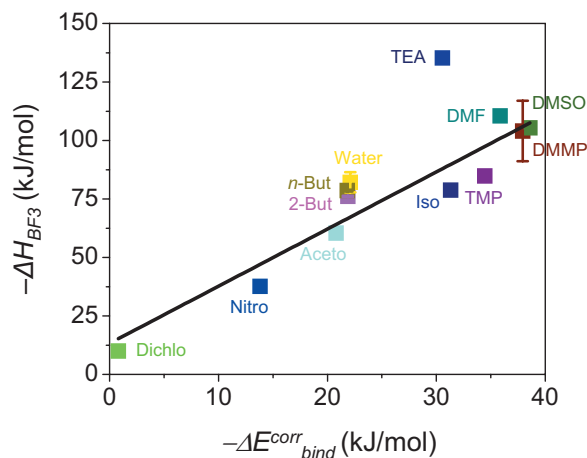


FIG. 3. (Color) Linear fit of Lewis basicities based on the $-\Delta H_{\text{BF}_3}$ enthalpy scale vs the DFT calculated adsorption energies $-\Delta E_{\text{bind}}^{\text{corr}}$. The linear fit shown omits TEA to give a slope of 2.44 and regression coefficient $R^2 = 0.88$. Including TEA in the fit lowers R^2 slightly to 0.73. Note that the binding energy value reported for TEA was obtained with the assistance of MD simulations as described in Sec. II. The error bars shown have been compiled using Ref. 24.

water are not available in the literature and hence were extrapolated from an exponential fit of sensor sensitivity data to $-\Delta H_{\text{BF}_3}$ values.¹²

The results of the DFT calculated adsorption energies for all 12 analytes binding to the Zn metal of the ZnPc monomer are plotted against Lewis basicity in Fig. 3. The least basic analyte (dichlo) is the weakest binder to ZnPc with a DFT calculated exothermicity of -0.81 kJ/mol. The DFT calculated binding strengths of the analytes to ZnPc increase as the analyte's basicity increases. For example, the basicities of 2-butanone (-76.07 kJ/mol) and DMF (-110.49 kJ/mol) are roughly two and three times greater than that of nitromethane (-37.63 kJ/mol) and their ZnPc binding strengths are also two and three times greater than nitromethane (-21.87 and -35.87 kJ/mol, respectively, versus -13.81 kJ/mol). Fitting the experimentally determined enthalpies of analyte complex formation to BF_3 versus DFT analyte binding strengths to ZnPc for all 12 analytes results in a linear dependence with a regression coefficient, $R^2 = 0.73$. The analyte binding energies are about a factor of 3 stronger to BF_3 than to ZnPc due to BF_3 being a stronger electron acceptor than ZnPc. Clearly, the outlier in the linear fit is TEA with a relatively weak binding strength to ZnPc (-30.49 kJ/mol) despite being the strongest base in the study (-135.87 kJ/mol). Omitting TEA from the fit results in a linear dependence between the analyte Lewis basicities and their coordination strengths to ZnPc with an improved $R^2 = 0.88$ and slope = 2.44.

Almost half of the analytes studied have a DFT binding strength to the Zn metal that is greater than the TEA-ZnPc DFT binding strength. The DFT calculations show that DMSO with a basicity of -105.34 ± 0.36 kJ/mol has the strongest binding to ZnPc with a -38.59 kJ/mol exothermicity of binding. Initially, the contrast between the weak binding strength of TEA with respect to its strong Lewis basicity was attributed to difficulties in obtaining the global minimum structure for the ZnPc-TEA complex instead of just a

local minimum structure. This initial hypothesis was consistent with the large number of degrees of freedom in the ZnPc-TEA complex; a large number of rotational configurations could be sampled as a result of rotation about the nitrogen-carbon and carbon-carbon σ -bonds of the TEA molecule. Geometry optimizations for six different ZnPc-TEA conformational isomers were sampled to give exothermic binding strengths ranging from -4.65 to -21.25 kJ/mol. Due to the large number of conformational isomers that could result from the ZnPc-TEA complex, MD simulations at 150 K were also incorporated in an attempt to obtain a more energetically favored ZnPc-TEA structure. The ZnPc-TEA structure obtained through performing MD simulations as described in Sec. II resulted in a structure that was 9.24 kJ/mol lower in energy than the most stable ZnPc-TEA configuration obtained only from G03 geometry optimizations. The lowest energy ZnPc-TEA structure is -30.49 kJ/mol exothermic; this value was used in the plot in Fig. 3. While this MD optimized structure is lower in energy than the structures that did not undergo a heating and cooling cycle, there still remains a large inconsistency in ZnPc binding energies for TEA compared to other less basic analytes investigated. This energy difference can be attributed to the steric effects of the ethyl groups on the TEA molecule upon binding to the Zn metal. This is consistent with numerous studies which have documented the steric effects of TEA.^{60,61} Unfortunately, higher temperature MD simulations which might provide further optimization are not practical since higher temperatures induce desorption suggesting experimental conditions cannot be accurately reproduced. As noted below, the ZnPc sensor response for TEA correlates poorly with the calculated TEA-ZnPc binding energy consistent with the inability of the subroom temperature DFT-MD simulation to fully capture the optimal binding configuration.

With the exception of TEA, ZnPc binding of the remaining analytes has a nearly linear correlation with their Lewis basicities. Since the basicity of a molecule is a measure of its ability to donate electrons, complexation of the 12 electron-donating analytes to the Zn metal may result in a transfer of electrons from the analyte to the ZnPc monomer. Charge transfer has been repeatedly cited as the mechanism in which MPc-based sensors operate.⁶²⁻⁶⁴ To determine the degree of charge transfer, the atomic charges of the ZnPc monomer and the ZnPc-analyte complexes were calculated using NPA calculations within the B3LYP functional and 6-31G* basis.⁶⁵ Mulliken charges were not used as they are notorious for their basis set dependence.^{66,67} The magnitude of charge transfer (Δq_{ZnPc}) is then determined by taking the difference of the total charge of the ZnPc molecule in the ZnPc-analyte complex minus the total charge of the ZnPc monomer. The charge transfer is plotted as a function of ZnPc binding strength, as shown in Fig. 4. The weakest binder dichloromethane results in a transfer of $0.014e^-$ to the ZnPc monomer, whereas the strongest binder DMSO results in the greatest transfer of electrons to the ZnPc monomer ($0.053e^-$). Regardless of where the analyte lies on the basicity scale, analyte adsorption onto the ZnPc monomer results in a small charge transfer from the analyte to the ZnPc; this is consistent with the electron donating nature of the basic analytes.

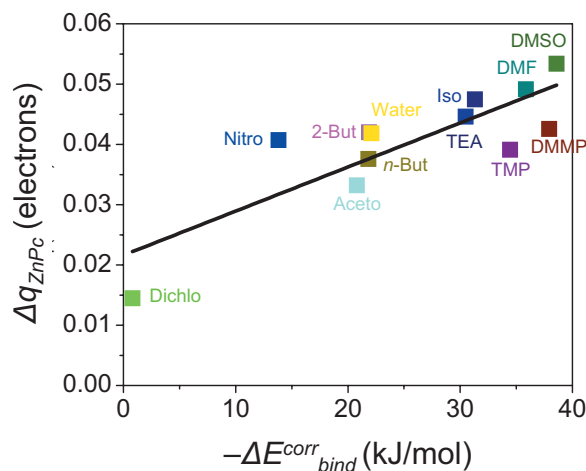


FIG. 4. (Color) A linear fit of the NPA calculated charge transfer after analyte adsorption (Δq_{ZnPc}) vs ZnPc binding energies ($-\Delta E_{\text{bind}}^{\text{corr}}$) to give a reasonable fit with $R^2=0.67$. Note that the small degree of charge transfer observed may be at the lower limits of the method. The charge transfer value reported for TEA was obtained from NPA calculations of the lowest energy TEA-ZnPc configuration obtained with the assistance of MD simulations as described in Sec. II.

The small charge transfer for these weakly bound analytes agrees with that observed in a previous study using the Bader charge analysis method that showed electron donating physisorbates donated $0.07e^-$ to the FePc metal center.^{23,68,69} Additionally, the analysis of the plot shows a modest linear dependence between the magnitude of electron donation from the analyte to the ZnPc monomer and their ZnPc binding energies ($R^2=0.67$). Although the DFT calculations show that charge transfer occurs on analyte binding to the Zn metal of the ZnPc monomer, this charge transfer is small and only a linear function of the binding energy. This is an important result because sensor response is a linear function of the analyte coverage and the charge transfer. Since the analyte coverage is an exponential function of analyte binding energy while the charge transfer is only a linear function of the analyte binding energy, the DFT calculations suggest that analyte sensitivities will be dominated by differences in analyte binding energies to the MPc instead of differences in charge transfer.

In sum, the magnitude of ZnPc binding strengths and limited charge transfer observed for these analytes suggest that the more basic analytes only weakly chemisorb, whereas the less basic analytes physisorb to the Zn metal center. In the case of dichloromethane, adsorption onto the Zn metal consists of weak physisorption. The small charge transfer is still consistent with ZnPc films being very sensitive to the presence of analytes because the films have low intrinsic carrier concentration and very weak surface doping by O_2 .⁷⁰⁻⁷²

B. ZnPc binding versus ZnPc chemiresistor sensor data

To investigate how analyte binding energies relate to experimental sensor data, the DFT calculated binding energies were compared to ZnPc sensor data. Details on chemiresistor sensor fabrication and device measurements can be found in

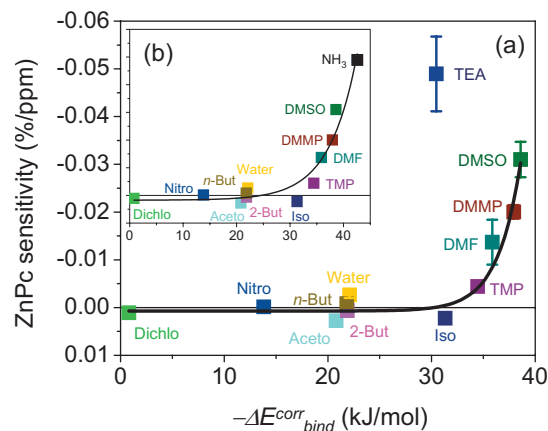


FIG. 5. (Color) (a) Curve of ZnPc sensitivities $[(\Delta I/I_{\text{baseline}} \times 100)/\text{analyte concentration}]$ vs $-\Delta E_{\text{bind}}^{\text{corr}}$ for all 12 analytes. The exponential fit shown omits TEA to give a good fit with $R^2=0.94$. Including TEA results in a poor exponential fit with $R^2=0.18$, clearly showing TEA is an outlier. Note that the binding energy value reported for TEA was obtained with the assistance of MD simulations as described in Sec. II. The error bars shown are a standard deviation of six slopes from the linear fit of ZnPc sensor response vs analyte concentration from Ref. 12. (b) The inset shows the same curve of ZnPc sensitivities vs $-\Delta E_{\text{bind}}^{\text{corr}}$ except the NH_3 -ZnPc binding strength has been substituted for the TEA-ZnPc binding strength. Substituting with NH_3 results in a good exponential fit with $R^2=0.93$.

Ref. 12. Briefly, the sensors are two-terminal interdigitated electrode devices consisting of Si (100) substrates with a $1 \mu\text{m}$ thick wet oxide. There are 45 electron beam evaporated gold finger pairs, each of which is spaced $5 \mu\text{m}$ apart with an electrode width and thickness of 2 nm and 45 nm , respectively. 50 nm thick ZnPc films were then deposited by organic molecular beam epitaxy. The sensor measurements were performed in a stainless steel chamber with SiO_2 passivated walls and an internal volume of 15 cm^3 . The sensor devices were operated at 8 V to ensure all measurements are done in the space-charge limited conductivity (SCLC) regime. Measurements performed within the SCLC regime are essential as it eliminates MPC/electrode interface effects on chemical sensing.⁷³ The sensors were exposed to analyte vapors at a $500 \text{ cm}^3/\text{min}$ flow rate of varying concentrations ranging from 90 to 900 ppm . It has been shown that a linear dependence between sensor response (percent current change $[\Delta I/I_{\text{baseline}} \times 100]$ at constant voltage) and analyte concentration exists in the region where the largest change in sensor current occurs upon analyte exposure. This region is considered the “initial fast region” and was systematically determined to occur within the first 5 min of dosing with analyte.¹³ As a result, all sensors were exposed to analyte vapors for 5 min to allow for a quantitative comparison of sensor response to analyte concentration. The relationship between sensor response and analyte concentration in the fast region was used to obtain ZnPc sensitivities (%/ppm) determined from the slope of the linear fits of response versus concentration. Additionally, it has been suggested that MPC sensor responses occurring within the first 5 min correspond to analyte adsorption onto metal centers free of atmospheric dopants such as O_2 .¹³ Therefore, the gas adsorption model used in this computational study, where the analyte adsorbs directly onto the Zn metal center of the ZnPc molecule, is an appropriate model system.

Figure 5(a) shows a plot of the experimentally determined ZnPc sensitivities versus the DFT calculated ZnPc binding energies for all 12 analytes. Note that positive sensitivities are for current gains while negative sensitivities are for current losses. In contrast to the linear dependence observed between analyte basicity and ZnPc binding strength, an exponential dependence exists for ZnPc sensitivities and binding strengths. An exponential dependence between sensitivity and binding strength is consistent with established models of surface coverage and binding energy. An exponential fit of all the data results in a poor regression coefficient $R^2=0.18$. Removal of TEA from the exponential fit results in a very good agreement between ZnPc sensitivities and binding strengths with $R^2=0.94$. As discussed above, steric effects adversely affect the calculated TEA binding to the Zn metal of the ZnPc molecule. To quantify the degree with which steric effects in TEA affect ZnPc binding in the DFT calculation, the binding strengths of two additional analytes, trimethylamine (TMA) and ammonia (NH_3), were also calculated using the methods discussed above. While TEA contains three bulky ethyl groups, TMA is less bulky with three methyl groups and NH_3 eliminates any possibility for steric hindrance to adversely affect the calculated ZnPc binding. The DFT calculations show that TMA binds to the Zn metal of ZnPc with an exothermic binding strength of -35.30 kJ/mol; this is almost 5 kJ/mol more exothermic than the calculated binding strength for TEA to ZnPc. NH_3 binding to ZnPc is even more exothermic with a calculated binding strength of -42.57 kJ/mol. These calculations show that TEA binding to ZnPc has severe steric constraints within the computational model. A plot of the experimentally determined ZnPc sensitivities versus the DFT calculated ZnPc binding energies where the NH_3 -ZnPc binding strength is substituted for the TEA-ZnPc binding strength can be found in Fig. 5(b). Exponentially fitting the plot with the NH_3 binding strength results in a good agreement with $R^2=0.93$. While TEA generally is a much weaker ligand than ammonia in coordination compounds,⁶¹ the relatively long weak bond to the metal center in MPc compounds will diminish the relative importance of steric crowding.

IV. CONCLUSIONS

DFT simulations were used to determine the binding strength of 12 electron donating analytes to the zinc metal of a ZnPc monomer. The analyte binding strengths were shown to be linearly dependent on their Lewis basicity based on the $-\Delta H_{\text{BF}_3}$ scale. NPA charge transfer calculations show that electron donating analyte complexation to ZnPc results in limited charge transfer from the analyte to the ZnPc monomer. The analyte sensitivities from chemiresistor ZnPc sensor data were proportional to an exponential of the binding energies from DFT calculations consistent with sensitivity being proportional to analyte coverage. The results show that MPc films can be employed for highly selective sensors since MPcs can even select for analytes with similar electronic properties because the response is an exponential function of the analyte binding energy. When an array of MPc sensors is employed, the small difference in binding strength

for a given analyte to the array of MPc films can be used to identify the analyte because the sensor response will depend exponentially on the analyte-MPc binding energy. In summary, the good correlation observed suggests that DFT is a reliable method to predict relative chemiresistor MPc analyte sensitivities.

ACKNOWLEDGMENTS

This research was supported in part by the National Science Foundation through TeraGrid resources provided by the San Diego Supercomputer Center (SDSC). The authors would like to thank AFOSR MURI (Grant No. F49620-02-1-0288) and NSF (Grant No. CHE-0350571) for funding of computational resources and the Department of Homeland Security for appointing N.L.T. to the U.S. Department of Homeland Security (DHS) Scholarship and Fellowship Program administered by the Oak Ridge Institute for Science and Education (ORISE) through an interagency agreement between the U.S. Department of Energy (DOE) and DHS. ORISE is managed by Oak Ridge Associated Universities (ORAU) under DOE Contract No. DE-AC05-06OR23100. All opinions expressed in this paper are the authors' and do not necessarily reflect the policies and views of DHS, DOE, or ORAU/ORISE. The authors would also like to thank Dr. Evgueni Chagarov for his guidance on performing the MD simulations for the ZnPc-TEA complex. Finally, N.L.T. would like to thank Professor M. E. Colvin for providing computational resources on GIGAN at UC Merced.

- ¹J. Buchholz and G. Somorjai, *J. Chem. Phys.* **66**, 573 (1977).
- ²P. Day, Z. Wang, and R. Pachter, *J. Mol. Struct.: THEOCHEM* **455**, 33 (1998).
- ³T. Gopakumar, M. Lackinger, M. Hackert, F. Muller, and M. Hietschold, *J. Phys. Chem. B* **108**, 7839 (2004).
- ⁴M. Liao and S. Scheiner, *J. Chem. Phys.* **114**, 9780 (2001).
- ⁵L. Lozzi, S. Santucci, and S. La Rosa, *Appl. Phys. Lett.* **88**, 133505 (2006).
- ⁶X. Lu and K. Hipps, *J. Phys. Chem. B* **101**, 5391 (1997).
- ⁷X. Lu, K. Hipps, X. Wang, and U. Mazur, *J. Am. Chem. Soc.* **118**, 7197 (1996).
- ⁸V. Mastryukov, C. Ruan, M. Fink, Z. Wang, and R. Pachter, *J. Mol. Struct.* **556**, 225 (2000).
- ⁹K. Nebesny, G. Collins, P. Lee, L. Chau, J. Danziger, E. Osburn, and N. Armstrong, *Chem. Mater.* **3**, 829 (1991).
- ¹⁰G. D. L. Torre, C. Claessans, and T. Torres, *Chem. Commun. (Cambridge)* **2006**, 2000.
- ¹¹B. Bott and T. Jones, *Sens. Actuators B* **5**, 43 (1984).
- ¹²F. I. Bohrer, C. N. Colesniuc, J. E. Park, M. E. Ruidaz, I. K. Schuller, A. C. Kummel, and W. C. Trogler, *J. Am. Chem. Soc.* **131**, 478 (2009).
- ¹³F. I. Bohrer, A. Sharoni, C. Colesniuc, J. Park, I. K. Schuller, A. C. Kummel, and W. C. Trogler, *J. Am. Chem. Soc.* **129**, 5640 (2007).
- ¹⁴R. D. Yang, J. E. Park, C. N. Colesniuc, I. K. Schuller, W. C. Trogler, and A. C. Kummel, *J. Chem. Phys.* **130**, 164703 (2009).
- ¹⁵J. Germain, A. Pauly, C. Maleysson, J. Blanc, and B. Schollhorn, *Thin Solid Films* **333**, 235 (1998).
- ¹⁶K. Morishige, S. Tomoyasu, and G. Iwano, *Langmuir* **13**, 5184 (1997).
- ¹⁷N. Ishikawa, D. Maurice, and M. HeadGordon, *Chem. Phys. Lett.* **260**, 178 (1996).
- ¹⁸K. Nguyen and R. Pachter, *J. Chem. Phys.* **114**, 10757 (2001).
- ¹⁹L. Lozzi, S. Santucci, S. La Rosa, B. Delley, and S. Picozzi, *J. Chem. Phys.* **121**, 1883 (2004).
- ²⁰T. Yamaguchi, *J. Phys. Soc. Jpn.* **66**, 749 (1997).
- ²¹B. Bialek, *Opt. Appl.* **35**, 323 (2005).
- ²²L. Lozzi, S. Picozzi, S. Santucci, C. Cantalini, and B. Delley, *J. Electron Spectrosc. Relat. Phenom.* **137-140**, 101 (2004).
- ²³N. Tran and A. Kummel, *J. Chem. Phys.* **127**, 214701 (2007).

- ²⁴ P. C. Maria and J. F. Gal, *J. Phys. Chem.* **89**, 1296 (1985).
- ²⁵ GAUSSIAN 03, Revision C.02, M. J. Frisch, G. W. Trucks, H. B. Schlegel, G. E. Scuseria, M. A. Robb, J. R. Cheeseman, J. A. Montgomery, Jr., T. Vreven, K. N. Kudin, J. C. Burant, J. M. Millam, S. S. Iyengar, J. Tomasi, V. Barone, B. Mennucci, M. Cossi, G. Scalmani, N. Rega, G. A. Petersson, H. Nakatsuji, M. Hada, M. Ehara, K. Toyota, R. Fukuda, J. Hasegawa, M. Ishida, T. Nakajima, Y. Honda, O. Kitao, H. Nakai, M. Klene, X. Li, J. E. Knox, H. P. Hratchian, J. B. Cross, V. Bakken, C. Adamo, J. Jaramillo, R. Gomperts, R. E. Stratmann, O. Yazyev, A. J. Austin, R. Cammi, C. Pomelli, J. W. Ochterski, P. Y. Ayala, K. Morokuma, G. A. Voth, P. Salvador, J. J. Dannenberg, V. G. Zakrzewski, S. Dapprich, A. D. Daniels, M. C. Strain, O. Farkas, D. K. Malick, A. D. Rabuck, K. Raghavachari, J. B. Foresman, J. V. Ortiz, Q. Cui, A. G. Baboul, S. Clifford, J. Cioslowski, B. B. Stefanov, G. Liu, A. Liashenko, P. Piskorz, I. Komaromi, R. L. Martin, D. J. Fox, T. Keith, M. A. Al-Laham, C. Y. Peng, A. Nanayakkara, M. Challacombe, P. M. W. Gill, B. Johnson, W. Chen, M. W. Wong, C. Gonzalez, and J. A. Pople, Gaussian, Inc., Wallingford, CT, 2004.
- ²⁶ A. D. Becke, *J. Chem. Phys.* **98**, 1372 (1993).
- ²⁷ C. T. Lee, W. T. Yang, and R. G. Parr, *Phys. Rev. B* **37**, 785 (1988).
- ²⁸ R. Ditchfield, W. Hehre, and J. Pople, *J. Chem. Phys.* **54**, 724 (1971).
- ²⁹ W. J. Hehre, R. Ditchfield, and J. A. Pople, *J. Chem. Phys.* **56**, 2257 (1972).
- ³⁰ N. Marom, O. Hod, G. E. Scuseria, and L. Kronik, *J. Chem. Phys.* **128**, 164107 (2008).
- ³¹ N. Marom and L. Kronik, *Appl. Phys. A: Mater. Sci. Process.* **95**, 165 (2009).
- ³² V. N. Nemykin, R. G. Hadt, R. V. Belosludov, H. Mizuseki, and Y. Kawazoe, *J. Phys. Chem. A* **111**, 12901 (2007).
- ³³ GaussView, Version 4.1, R. Dennington II, T. Keith, and J. Millam, Semichem, Inc., Shawnee Mission, KS, 2007.
- ³⁴ C. Y. Ruan, V. Mastryukov, and M. Fink, *J. Chem. Phys.* **111**, 3035 (1999).
- ³⁵ T. Visentin, E. Kochanski, and A. Dedieu, *J. Mol. Struct.: THEOCHEM* **431**, 255 (1998).
- ³⁶ C. W. Bock, S. V. Krasnoshchiokov, L. V. Khristenko, Y. N. Panchenko, and Y. A. Pentin, *J. Mol. Struct.: THEOCHEM* **34**, 201 (1987).
- ³⁷ D. Begue, P. Carbonniere, and C. Pouchan, *J. Phys. Chem. A* **109**, 4611 (2005).
- ³⁸ P. Raeymaekers, H. Figeys, and P. Geerlings, *J. Mol. Struct.: THEOCHEM* **46**, 509 (1988).
- ³⁹ H. Z. Zhong, E. L. Stewart, M. Kontoyianni, and J. P. Bowen, *J. Chem. Theory Comput.* **1**, 230 (2005).
- ⁴⁰ K. K. Irikura and J. F. Liebman, <http://webbook.nist.gov/chemistry/3d-structs/>, 1998–1999.
- ⁴¹ L. George, K. S. Viswanathan, and S. Singh, *J. Phys. Chem. A* **101**, 2459 (1997).
- ⁴² R. D. Suenram, F. J. Lovas, D. F. Plusquellic, A. Lesarri, Y. Kawashima, J. O. Jensen, and A. C. Samuels, *J. Mol. Spectrosc.* **211**, 110 (2002).
- ⁴³ V. M. Lynch, S. N. Thomas, S. H. Simonsen, T. V. Rao, G. K. Trivedi, and S. K. Arora, *Acta Crystallogr., Sect. C: Cryst. Struct. Commun.* **45**, 169 (1989).
- ⁴⁴ V. Typke and M. Dakkouri, *J. Mol. Struct.* **599**, 177 (2001).
- ⁴⁵ G. Schultz and I. Hargittai, *J. Phys. Chem.* **97**, 4966 (1993).
- ⁴⁶ M. Tanaka and M. Aida, *Chem. Phys. Lett.* **417**, 316 (2006).
- ⁴⁷ S. Wei, W. B. Tzeng, and A. W. Castleman, *J. Phys. Chem.* **94**, 6927 (1990).
- ⁴⁸ S. Bishop, N. Tran, G. Poon, and A. Kummel, *J. Chem. Phys.* **127**, 214702 (2007).
- ⁴⁹ N. L. Tran, S. R. Bishop, T. J. Grassman, G. C. Poon, F. I. Bohrer, W. C. Trogler, and A. C. Kummel, *J. Chem. Phys.* **130**, 174305 (2009).
- ⁵⁰ J. D. Wright, *Prog. Surf. Sci.* **31**, 1 (1989).
- ⁵¹ See EPAPS Document No. E-JCPSA6-130-001921 for the most stable ZnPc-DMF and ZnPc-analyte conformations. For more information on EPAPS, see <http://www.aip.org/pubservs/epaps.html>.
- ⁵² G. Kresse and J. Furthmuller, *Comput. Mater. Sci.* **6**, 15 (1996).
- ⁵³ G. Kresse and J. Furthmuller, *Phys. Rev. B* **54**, 11169 (1996).
- ⁵⁴ G. Kresse and J. Hafner, *J. Phys.: Condens. Matter* **6**, 8245 (1994).
- ⁵⁵ J. Perdew, K. Burke, and M. Ernzerhof, *Phys. Rev. Lett.* **77**, 3865 (1996).
- ⁵⁶ D. Vanderbilt, *Phys. Rev. B* **41**, 7892 (1990).
- ⁵⁷ S. F. Boys and F. Bernardi, *Mol. Phys.* **19**, 553 (1970).
- ⁵⁸ S. Simon, M. Duran, and J. J. Dannenberg, *J. Chem. Phys.* **105**, 11024 (1996).
- ⁵⁹ W. A. Herrebout and B. J. vanderVeken, *J. Am. Chem. Soc.* **119**, 10446 (1997).
- ⁶⁰ H. C. Brown and S. Sujishi, *J. Am. Chem. Soc.* **70**, 2878 (1948).
- ⁶¹ A. L. Seligson and W. C. Trogler, *J. Am. Chem. Soc.* **113**, 2520 (1991).
- ⁶² M. Bouvet, G. Guillaud, A. Leroy, A. Maillard, S. Spirkovitch, and F. Tourmilhac, *Sens. Actuators B* **73**, 63 (2001).
- ⁶³ R. Gould, *Coord. Chem. Rev.* **156**, 237 (1996).
- ⁶⁴ R. D. Gould and N. A. Ibrahim, *Thin Solid Films* **398–399**, 432 (2001).
- ⁶⁵ A. E. Reed, R. B. Weinstock, and F. Weinhold, *J. Chem. Phys.* **83**, 735 (1985).
- ⁶⁶ C. Cramer, *Essentials of Computational Chemistry: Theories and Models*, 1st ed. (Wiley, New York, 2002).
- ⁶⁷ F. Jensen, *Introduction to Computational Chemistry*, 1st ed. (Wiley, New York, 1999).
- ⁶⁸ R. Bader, *Atoms in Molecules: A Quantum Theory* (Oxford University Press, New York, 1990).
- ⁶⁹ G. Henkelman, A. Arnaldsson, and H. Jonsson, *Comput. Mater. Sci.* **36**, 354 (2006).
- ⁷⁰ E. v. Faassen and H. Kerp, *Sens. Actuators B* **88**, 329 (2003).
- ⁷¹ H. Kerp, K. Westerduin, A. T. van Veen, and E. van Faassen, *J. Mater. Res.* **16**, 503 (2001).
- ⁷² M. Passard, A. Pauly, J. Blanc, S. Dogo, J. Germain, and C. Maleysson, *Thin Solid Films* **237**, 272 (1994).
- ⁷³ K. Miller, R. Yang, M. Hale, J. Park, B. Fruhberger, C. Colesniuc, I. Schuller, A. Kummel, and W. Trogler, *J. Phys. Chem. B* **110**, 361 (2006).